Beta thalassemia minor is a beneficial determinant of red blood cell storage lesion

Vassilis L. Tzounakas,[1*] Alkmini T. Anastasiadi,[1*] Davide Stefanoni,[2] Francesca Cendali,[2] Lorenzo Bertolone,[2] Fabia Gamboni,[2] Monika Dzieciatkowska,[2] Pantelis Rousakis,[3] Athina Vergaki,[4] Vassilis Soulakis,[4] Ourania E. Tsitsilonis,[3] Konstantinos Stamoulis,[5] Issidora S. Papassideri,[1] Anastasios G. Kriebardis,[6] Angelo D'Alessandro[2] and Marianna H. Antonelou[1]

[1]Department of Biology, Section of Cell Biology and Biophysics, School of Science, National and Kapodistrian University of Athens (NKUA), Athens, Greece; [2]Department of Biochemistry and Molecular Genetics, University of Colorado, School of Medicine–Anschutz Medical Campus, Aurora, CO, USA; [3]Department of Biology, Section of Animal and Human Physiology, School of Science (NKUA), Athens, Greece; [4]Regional Blood Transfusion Center, "Agios Panteleimon" General Hospital of Nikea, Piraeus, Greece; [5]Hellenic National Blood Transfusion Center, Acharnes, Athens, Greece and [6]Department of Biomedical Science, School of Health & Caring Science, University of West Attica (UniWA), Egaleo, Greece.

**VLT and ATA contributed equally as co-first authors.*

 doi:10.3324/haematol.2020.273946

Received: October 6, 2020.

Accepted: December 4, 2020.

Pre-published: March 18, 2021.

Correspondence: *MARIANNA H. ANTONELOU* - manton@biol.uoa.gr

ANGELO D'ALESSANDRO - angelo.dalessandro@cuanschutz.edu

Regular Article

Beta-thalassemia minor is a beneficial determinant of red blood cell storage lesion

[*]Vassilis L. Tzounakas,[1] [*]Alkmini T. Anastasiadi,[1] Davide Stefanoni,[2] Francesca Cendali,[2] Lorenzo Bertolone,[2] Fabia Gamboni,[2] Monika Dzieciatkowska,[2] Pantelis Rousakis,[3] Athina Vergaki,[4] Vassilis Soulakis,[4] Ourania E. Tsitsilonis,[3] Konstantinos Stamoulis,[5] Issidora S. Papassideri,[1] Anastasios G. Kriebardis,[6] [**]Angelo D'Alessandro,[2] [**]Marianna H. Antonelou[1]

[1]Department of Biology, Section of Cell Biology and Biophysics, School of Science, National and Kapodistrian University of Athens (NKUA), Athens, Greece;
[2] Department of Biochemistry and Molecular Genetics, University of Colorado, School of Medicine–Anschutz Medical Campus, Aurora, CO, USA;
[3]Department of Biology, Section of Animal and Human Physiology, School of Science, NKUA, Athens, Greece;
[4]Regional Blood Transfusion Center, "Agios Panteleimon" General Hospital of Nikea, Piraeus, Greece;
[5]Hellenic National Blood Transfusion Centre, Acharnes, Athens, Greece;
[6]Department of Biomedical Science, School of Health & Caring Science, University of West Attica (UniWA), Egaleo, Greece.

(**) Corresponding Authors: (1) Marianna H. Antonelou, Department of Biology, National & Kapodistrian University of Athens (NKUA), Panepistimiopolis Zografou, Athens 15784, Greece; e-mail: manton@biol.uoa.gr (2) Angelo D'Alessandro, Department of Biochemistry and Molecular Genetics, University of Colorado, School of Medicine–Anschutz Medical Campus, Aurora, 80045 CO, USA angelo.dalessandro@cuanschutz.edu

(*) VLT and ATA are co-first authors

Running Heads: The favorable storability of βThal^{+} RBCs
Word count: Text (3933), Abstract (250)
Tables: 1
Figures: 7
References: 50
Supplementary Files: 1

Acknowledgements: This project has received funding from the Hellenic Foundation for Research and Innovation (HFRI) and the General Secretariat for Research and Technology (GSRT), under grant agreement No 2032 (VLT).

Disclosure of Conflict of Interest: Though unrelated to the contents of this manuscript, ADA declares that he is a founder of Omix Technologies Inc and Altis Biosciencens LLC and a consultant for Hemanext Inc.

Table of Contents

Supplementary Methods

Haematological/biochemical Parameters

Haematological analysis was performed using the automatic blood cell counters BC-3000 PLUS, MINDRAY Celltac E, MEK-7222 K, NIHON KOHDEN. Double measurements were performed to achieve maximum reliability. Biochemical analysis of triglycerides, cholesterol, lipoproteins, iron (Fe), potassium (K^+), sodium (Na^+) etc. was performed using the automatic analyzers Hitachi 902, AVL Series Electrolyte Analyzer 9180 and Elecsys Systems Analyzer (Roche).

Redox parameters, Calcium accumulation and Phosphatidylserine (PS) exposure

The ferric reducing antioxidant power (FRAP) assay was used to determine total (TAC), uric acid (UA) dependent (UAdAC) and UA independent (UAiAC) antioxidant capacities of plasma/supernatant,[1] with/without uricase (Sigma Aldrich, Munich, Germany) treatment[2]. For membrane lipid peroxidation assessment, RBCs were treated with 20% trichloroacetic acid and then with 0.67% thiobarbituric acid (TBA, 50min at 90°C) that produces a chromogenic complex with malondialdehyde (MDA), a widely accepted biomarker of lipid peroxidation[3]. Intracellular accumulation of reactive oxygen species (ROS) and calcium (Ca^{2+}) was estimated by fluorometry using the membrane permeable acetyl ester CM-H_2DCFDA and the calcium indicator Fluo-4 AM (Invitrogen, Molecular Probes, Eugene, OR), respectively. ROS generation was also measured following RBC stimulation by tert-butyl-hydroperoxide (tBHP; 100μM), diamide (2 mM) and PHZ (100 μM) for 45min at 37°C. Phosphatidylserine (PS) exposure was estimated by multicolor flow cytometry following labeling of RBCs with phycoerythrin (PE)-Annexin V and fluorescein isothiocyanate (FITC)-conjugated anti-CD235 antibody (BD Pharmingen, San Jose, CA) in isotonic Hepes buffer pH 7.4, containing 2.5 mM calcium. Cells analyzed in a FACSCanto II instrument equipped with the FACSDiva software (Becton Dickinson San Jose, CA) with isotype matched FITC/PE-antibodies, as previously reported[4].

RBC fractionation and Immunoblotting

RBC membranes were isolated by hypotonic lysis of RBCs in 5 mmol/L sodium phosphate buffer (pH 8.0)[4]. For detection of protein carbonylation the Oxyblot detection kit was used as per manufacturer's specifications. The protein bands were detected by chemiluminescence and quantified by scanning densitometry.

Omics analyses

Preliminary proteomics analyses were performed in stored samples of RBC membranes through a FASP digestion prior to analysis via nano-UHPLC-MS/MS[5] (Evosep One system coupled to timsTOF Pro mass spectrometer - Bruker Daltonics, Bremen, Germany), as extensively described in prior technical notes[6]. Metabolomics analyses were performed as previously reported[7]. 100 μL of stored RBCs were collected on a weekly basis, extracted at 1:6 dilution in methanol:acetonitrile:water (5:3:2) and analyzed by UHPLC-MS (Ultimate 3000 RSLC-Q Exactive, Thermo Fisher). Sample extracts (10 μL) were loaded onto a Kinetex XB-C18 column (150 mm × 2.1 mm × 1.7 μm—Phenomenex, Torrance, CA, USA). A 5-min

gradient from 5 to 95% B (phase A: water + 0.1% formic acid and B: acetonitrile + 0.1% formic acid) eluted metabolites into a Q Exactive system (Thermo, Bremen, Germany), scanning in full MS mode or performing acquisition independent fragmentation (MS/MS analysis—5 min method) at 70,000 resolution in the 60–900 m/z range, 4 kV spray voltage, 15 sheath gas, and 5 auxiliary gas, operated in negative and then positive ion mode (separate runs). Metabolite assignment was performed against an in house standard library, as reported[8], through the freely available software Maven (Princeton University, USA)[9]. No data pre-processing (neither normalization nor log-transformation) was performed.

Supplementary Tables

Supplementary Table S1. Blood donor demographics and haematological characteristics.

	Control (n=20)	ϐThal^{+} (n=18)
Sex (M/F)	16/4	15/3
Age (y)	38±14	40±10
Origin	Greek	Greek
Blood Group (A/B/O)	9/2/9	5/0/13
Rhesus (+/-)	17/3	14/4
Smoking (Y/N)	10/10	10/8
Donation Frequency/Year	1.72±0.46	1.63±0.67
Red blood cells (RBC) (x10^6/μL)	5.05±0.35	6.48±0.49*
Haematocrit (Hct) (%)	43.70±3.77	42.58±2.32
Total Haemoglobin (Hb) (g/dL)	14.49±1.45	13.93±0.53
Mean corpuscular volume (MCV) (fL)	86.67±6.34	65.59±6.26*
Mean corpuscular Hb (MCH) (pg)	28.72±2.32	21.16±2.36*
Mean corpuscular Hb concentration (MCHC) (g/dL)	33.13±1.31	32.21±1.18
Red cell distribution width (RDW) (%)	13.36±1.33	15.84±2.16*
White blood cells (WBC) (x10^3/μL)	7.27±2.07	7.55±1.47
Platelet count (x10^3/μL)	255±52	230±41
Plateletcrit (PCT) (%)	0.26±0.08	0.24±0.05
Mean platelet volume (MPV) (fL)	10.22±1.59	10.67±1.30
Glycated Hb (HbA_{1c}) (%)	4.94±0.35	5.17±0.40
Haemoglobin A_2 (HbA_2) (%)	2.50±0.66	4.80±0.63*

Age. donation frequency per year and haematological parameters are presented as mean±SD. (*) $p<0.05$

Supplementary Table S2. Abbreviations and annotations used in the biological networks shown in Figure 8.

Parameter	Abbreviation
Mean corpuscular fragility	MCF
Total antioxidant capacity	TAC
Uric acid-independent antioxidant capacity	UAiAC
Uric acid-dependent antioxidant capacity	UAdAC
Linoleoyl CoA	1
Acetyl carnitine	2
Isovalerylcarnitine	3
4Acyl C5 OH	4
L-octanoylcarnitine	5
ADP	6
Alpha-D-Ribose 1-phosphate	7
AMP	8
Ascorbate	9
Band 3 fragmentation*	10
Band 3 clustering*	11
1-4-beta-D-Xylan	12
Butanoic acid	13
Citrate	14
CMP	15
CMP-N-acetylneuraminate	16
Creatinine	17
Cytidine	18
Cytosine	19
D-Erythrose 4-phosphate	20
D-glucose	21
D-Glucose-6-phosphate	22
dAMP	23
Decanoic acid (caprate)	24
Dehydroascorbate	25
Diamide-induced reactive oxygen species	26
5-6-Dihydrothymine	27
Dimethylglycine	28
Eicosapentaenoic acid	29
Plasma/supernatant Free Hb	30
Fumarate	31
Gamma-L-Glutamyl-D-alanine	32
Gamma-L-Glutamyl-L-cysteine	33
GDP	34
Guanidinoacetate	35
Guanine	36

Total Hb (g/dL)	37
Membrane-bound Hb*	38
Glycated Hb (HbA1c)	39
Haemoglobin A_2 (HbA_2)	40
Haematocrit (Hct)	41
Hexadecenoic acid	42
5-Hydroxyisourate	43
Hypotaurine	44
IMP	45
Itaconate	46
Kynurenine	47
(5-L-Glutamyl)-L-glutamine	48
L-arginine	49
L-aspartate	50
L-cysteate	51
L-homocysteine	52
L-serine	53
Lactate	54
Malate	55
Maltose	56
Mannitol	57
Mean corpuscular Hb (MCH)	58
2- Methyleneglutarate	59
Mechanical fragility index	60
Mean platelet volume (MPV)	61
N-Acetylneuraminate	62
Octadecanoic acid	63
Ornithine	64
Oxaloacetate	65
2-Oxoglutarate	66
Oxidative haemolysis	67
Pantetheine	68
Pantothenol	69
Pentanoate (valerate)	70
5-Phospho-alpha-D-ribose 1-diphosphate	71
6-Phospho-D-gluconate	72
Phosphocreatine	73
Phenylhydrazine-induced reactive oxygen species	74
Platelet count (PCT)	75
Membrane bound peroxiredoxin-2*	76
Pyruvate	77
Red cell distribution width (RDW)	78
S-Allantoin	79

S-Glutathiony-L-cysteine	80
Membrane-bound clusterin*	81
Sedoheptulose-1-phosphate	82
Sn-glycero-3-Phosphoethanolamine	83
Sphingosine-1-phosphate	84
Succinate	85
Tetradecenoic acid	86
Trans-4-Hydroxy-L-proline	87
Transferin	88
UDP-glucose	89
UDP-N-acetyl-D-glucosamine	90
Urate	91
5Z-8Z-11Z-14Z-17Z-Icosapentaenoic acid	92
8Z-11Z-14Z-Icosatrienoic acid	93
Extracellular potassium	94

"s" after abbreviations or numbers in the biological networks stands for values in stored samples. (*) data not shown.

Supplementary Figures

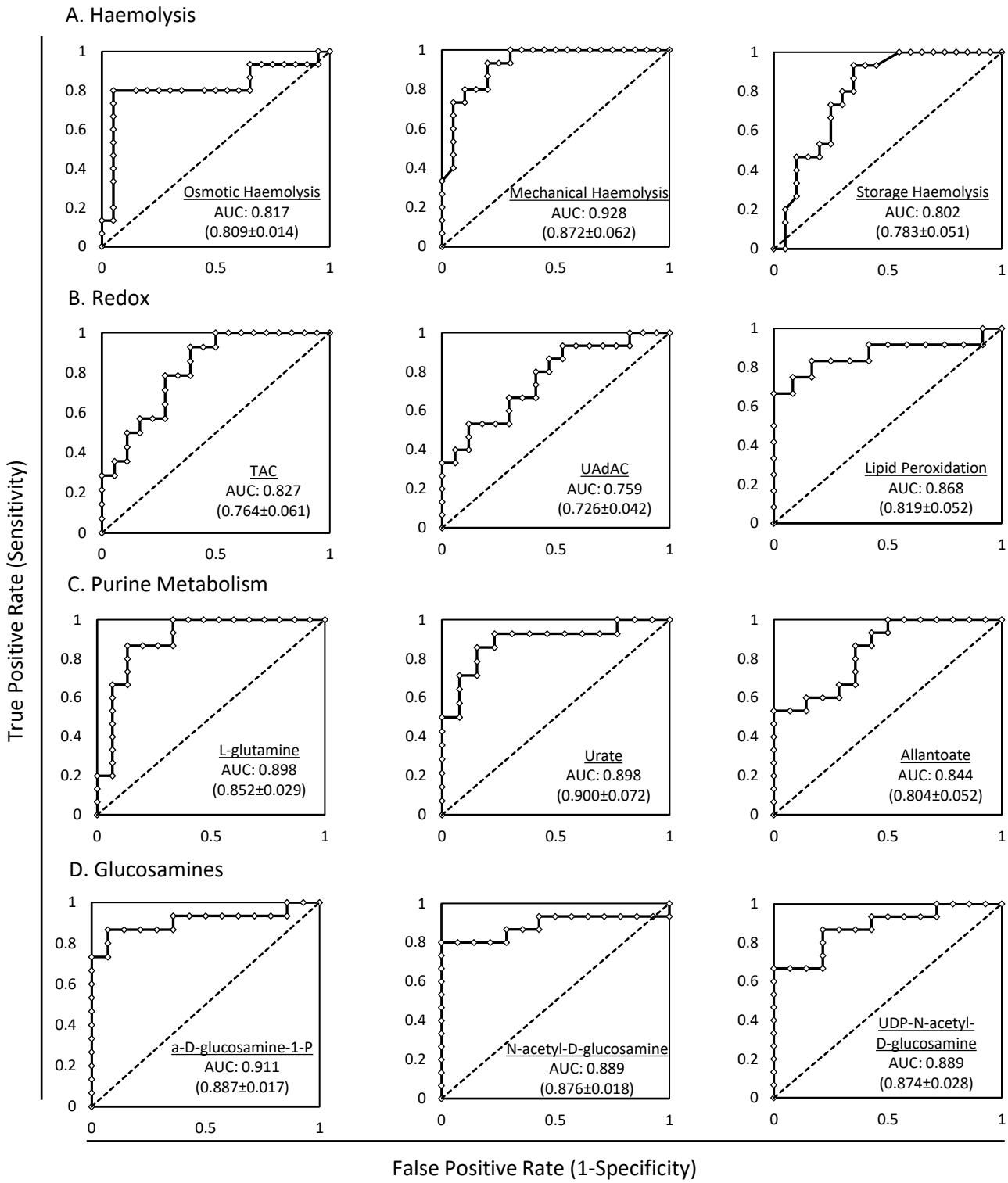

Supplementary Figure S1. Receiver operating characteristic (ROC) curves that predict beta-thalassaemia minor (βThal$^+$) stored RBCs. Representative ROC curves for selected storage (A) haemolysis, (B) redox, (C) purine metabolism and (D) glucosamine metabolism parameters. Only curves for the middle storage are shown, however similar statistically significant results were observed for every storage period measured, except for uric acid dependent antioxidant capacity (UAdAC) and free Hb (1 statistically insignificant time point for each variable). Data are presented as area under the curve (AUC) for each parameter, plus mean AUC ± SD for the whole storage period. TAC: total antioxidant capacity of the supernatant of blood units; dashed line: reference line.

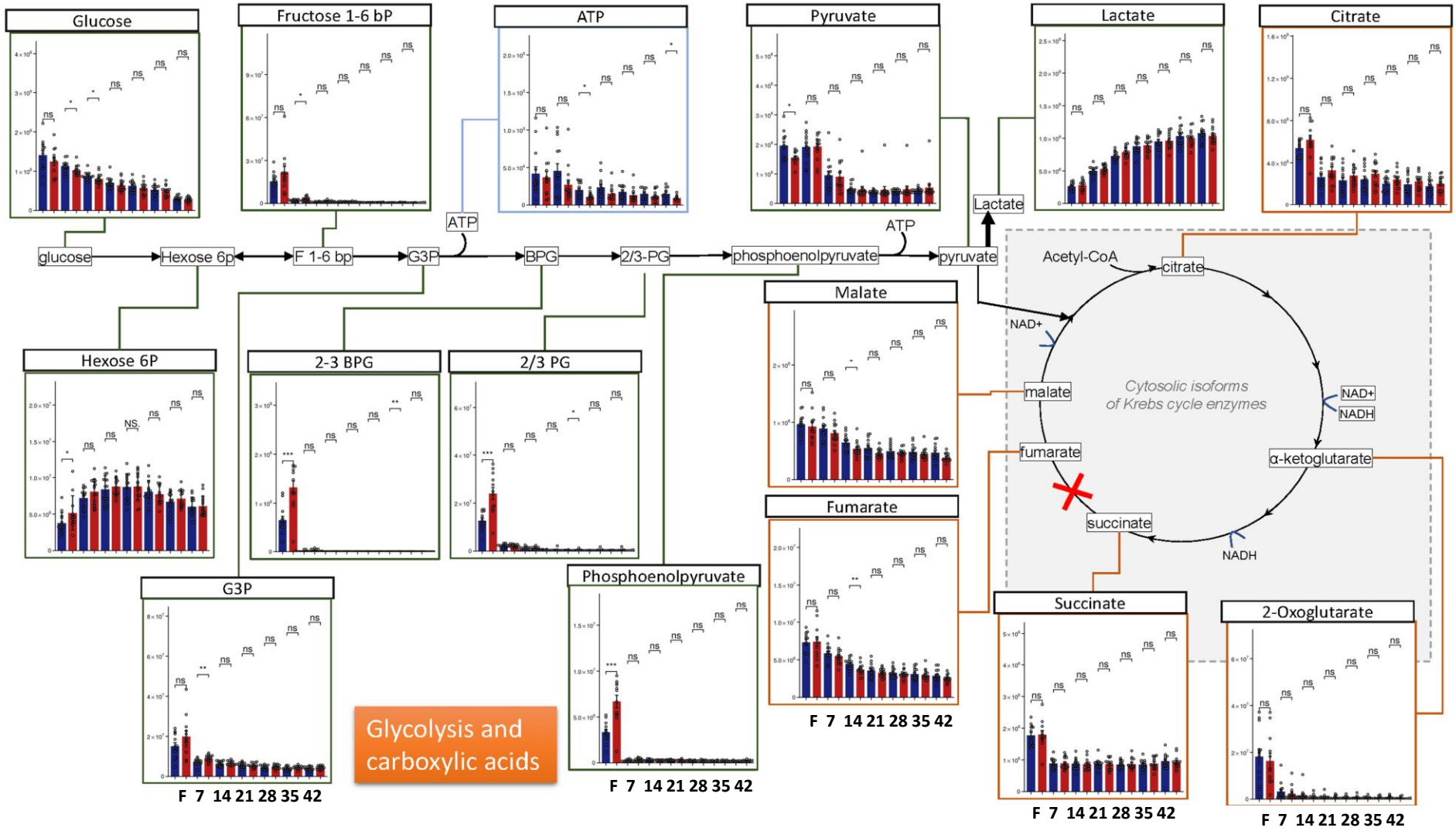

Supplementary Figure S2. Bar plots of metabolites in glycolysis and carboxylic acids in control (blue) and βThal⁺ (red) RBCs *in vivo* (fresh blood, F) and weekly through storage (days 7, 14, 21, 28, 35 and 42). ns: non-statistically significant difference. (*), (**), (***): p< 0.05, 0.01, 0.001 βThal⁺ vs. control, respectively.

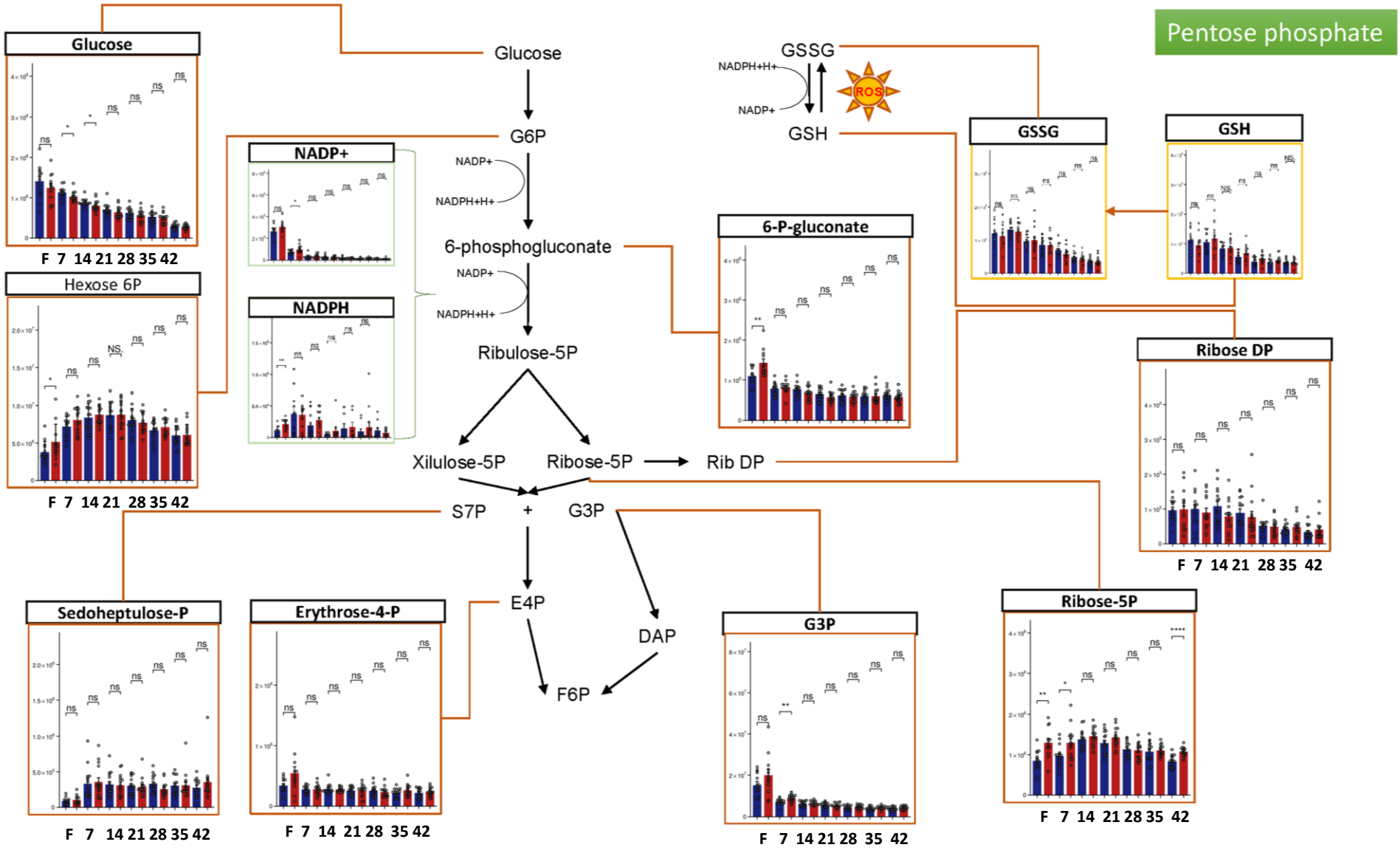

Supplementary Figure S3. Bar plots of metabolites in the pentose phosphate pathway and glutathione homeostasis in control (blue) and βThal$^+$ (red) RBCs *in vivo* (fresh blood, F) and weekly through storage (days 7, 14, 21, 28, 35 and 42). (*), (**), (***), (****): p< 0.05, 0.01, 0.001, 0.0001 βThal$^+$ vs. control, respectively.

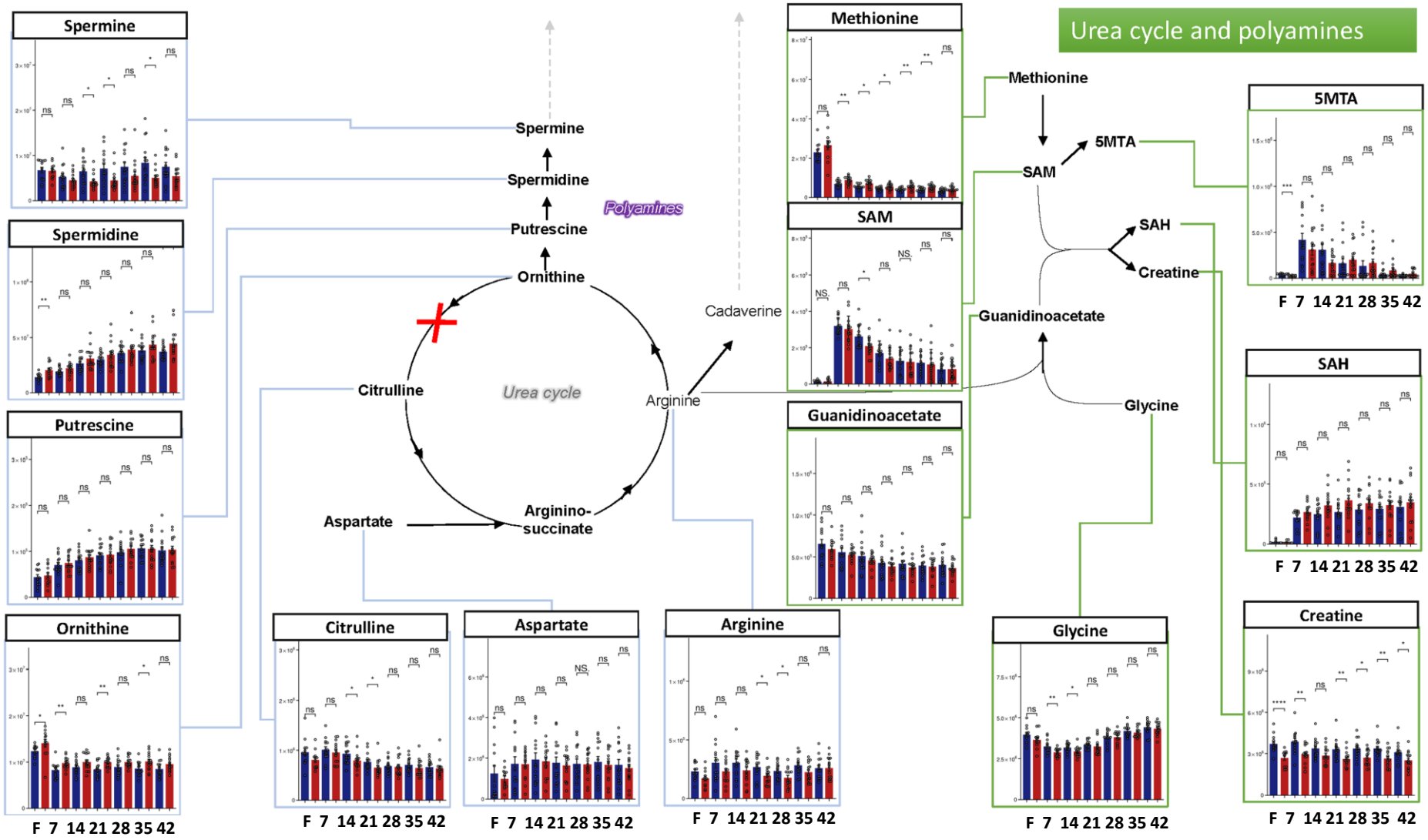

Supplementary Figure S4. Bar plots of metabolites in arginine and methionine metabolism in control (blue) and ϐThal^{+} (red) RBCs *in vivo* (fresh blood, F) and weekly through storage (days 7, 14, 21, 28, 35 and 42). (*), (**), (***), (****): p< 0.05, 0.01, 0.001, 0.0001 ϐThal^{+} vs. control, respectively.

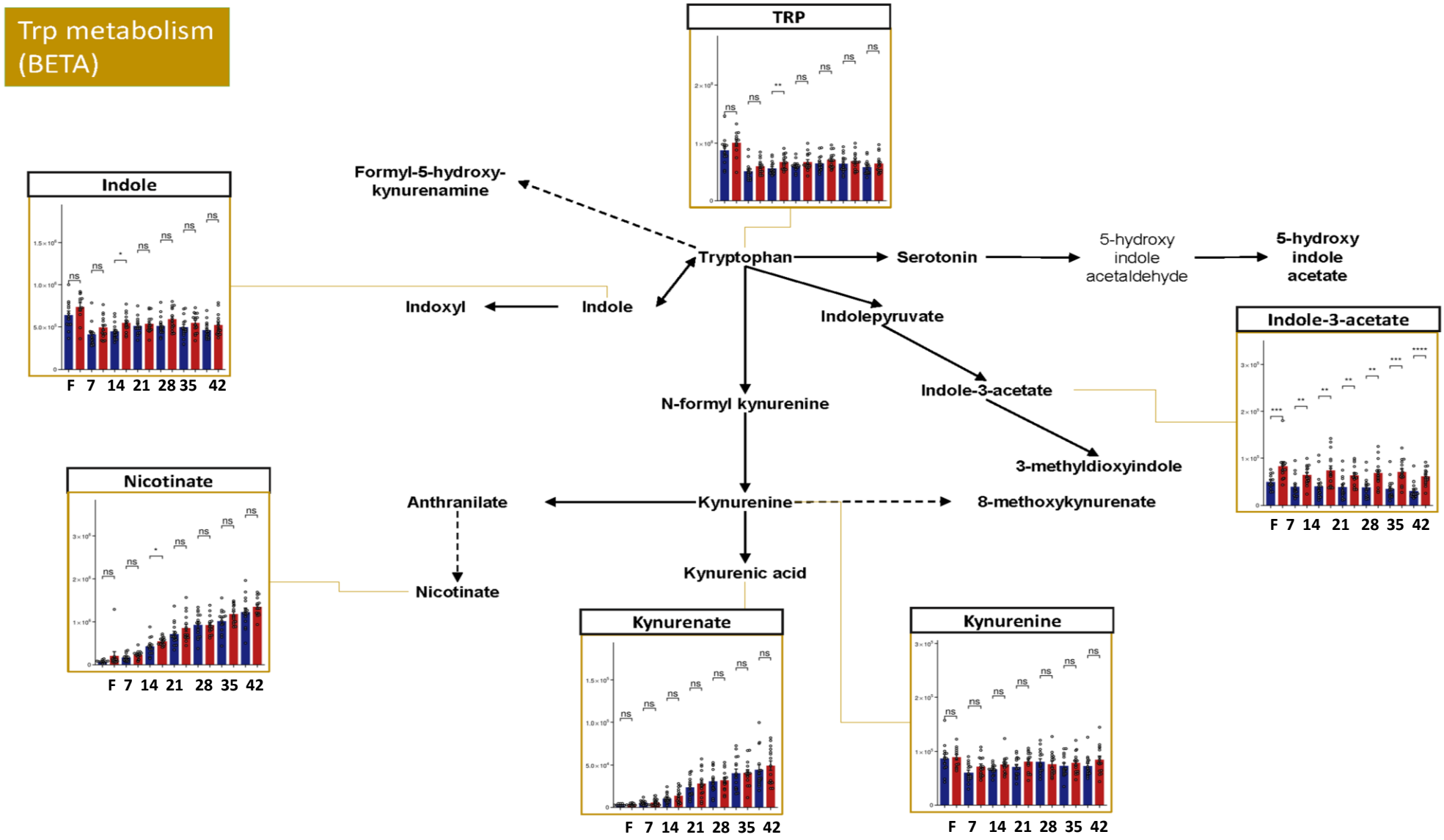

Supplementary Figure S5. Bar plots of metabolites in tryptophan pathway in control (blue) and beta-thalassaemia (red) RBCs *in vivo* (fresh blood, F) and weekly through storage (days 7, 14, 21, 28, 35 and 42). (*), (**), (***), (****): p< 0.05, 0.01, 0.001, 0.0001 βThal^{+} vs. control, respectively.

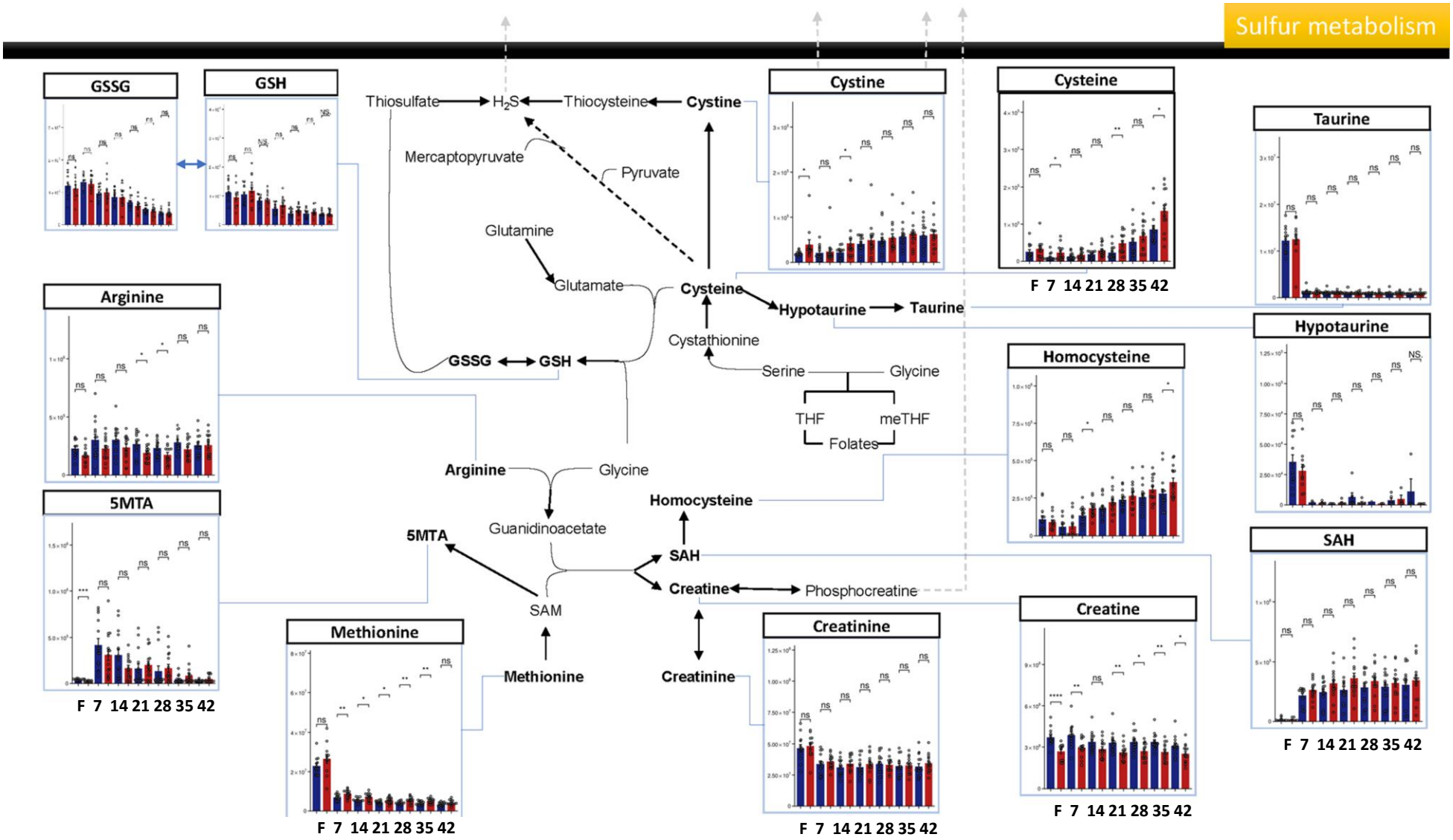

Supplementary Figure S6. Bar plots of metabolites in sulfur and arginine pathways in control (blue) and βThal⁺ (red) RBCs *in vivo* (fresh blood, F) and weekly through storage (days 7, 14, 21, 28, 35 and 42). (*), (**), (***), (****): p< 0.05, 0.01, 0.001, 0.0001 βThal⁺ vs. control, respectively.

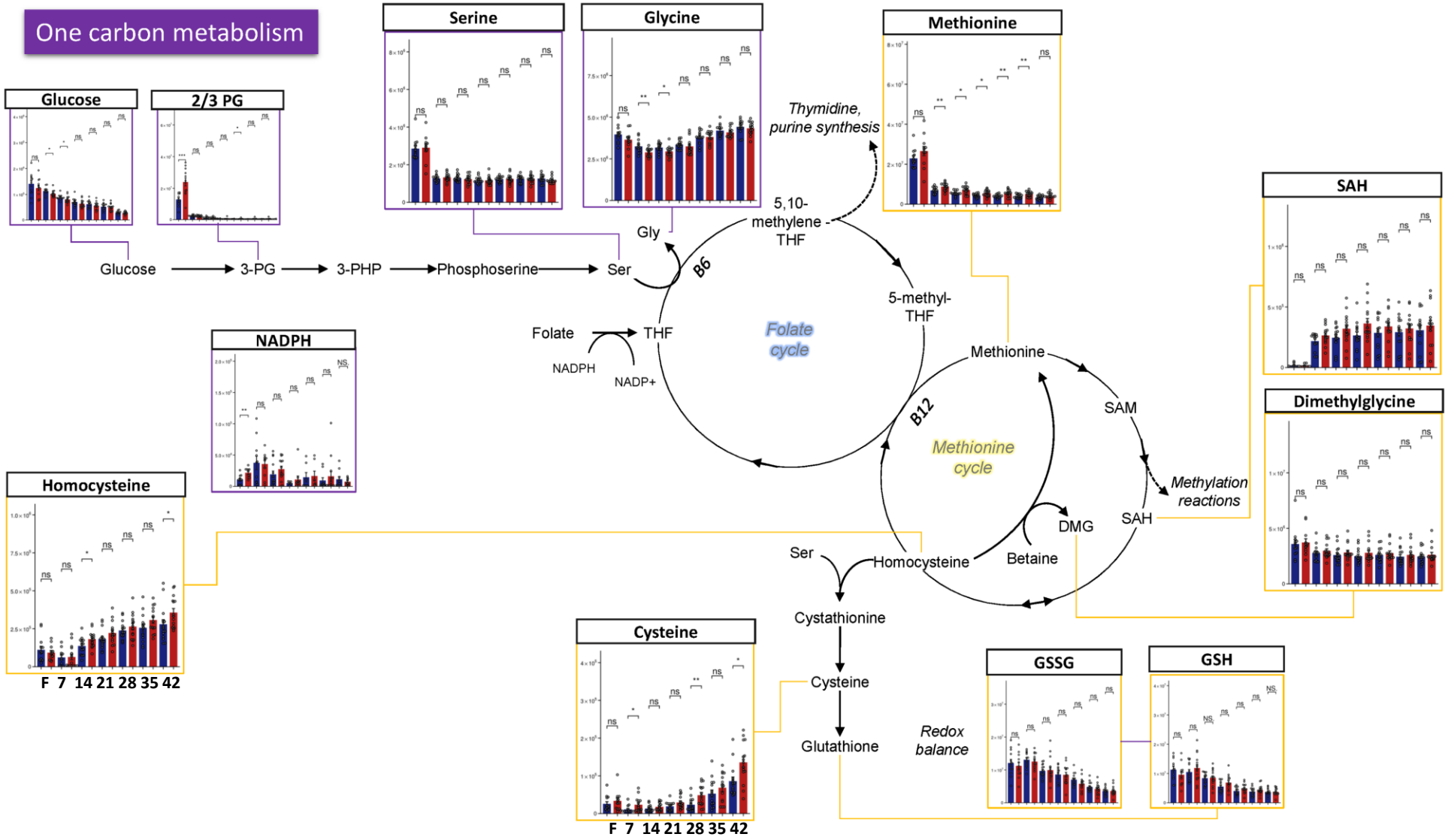

Supplementary Figure S7. Bar plots of components of one-carbon metabolic pathways in control (blue) and βThal^{+} (red) RBCs *in vivo* (fresh blood, F) and weekly through storage (days 7, 14, 21, 28, 35 and 42). (*), (**): p< 0.05, 0.01 βThal^{+} vs. control, respectively.

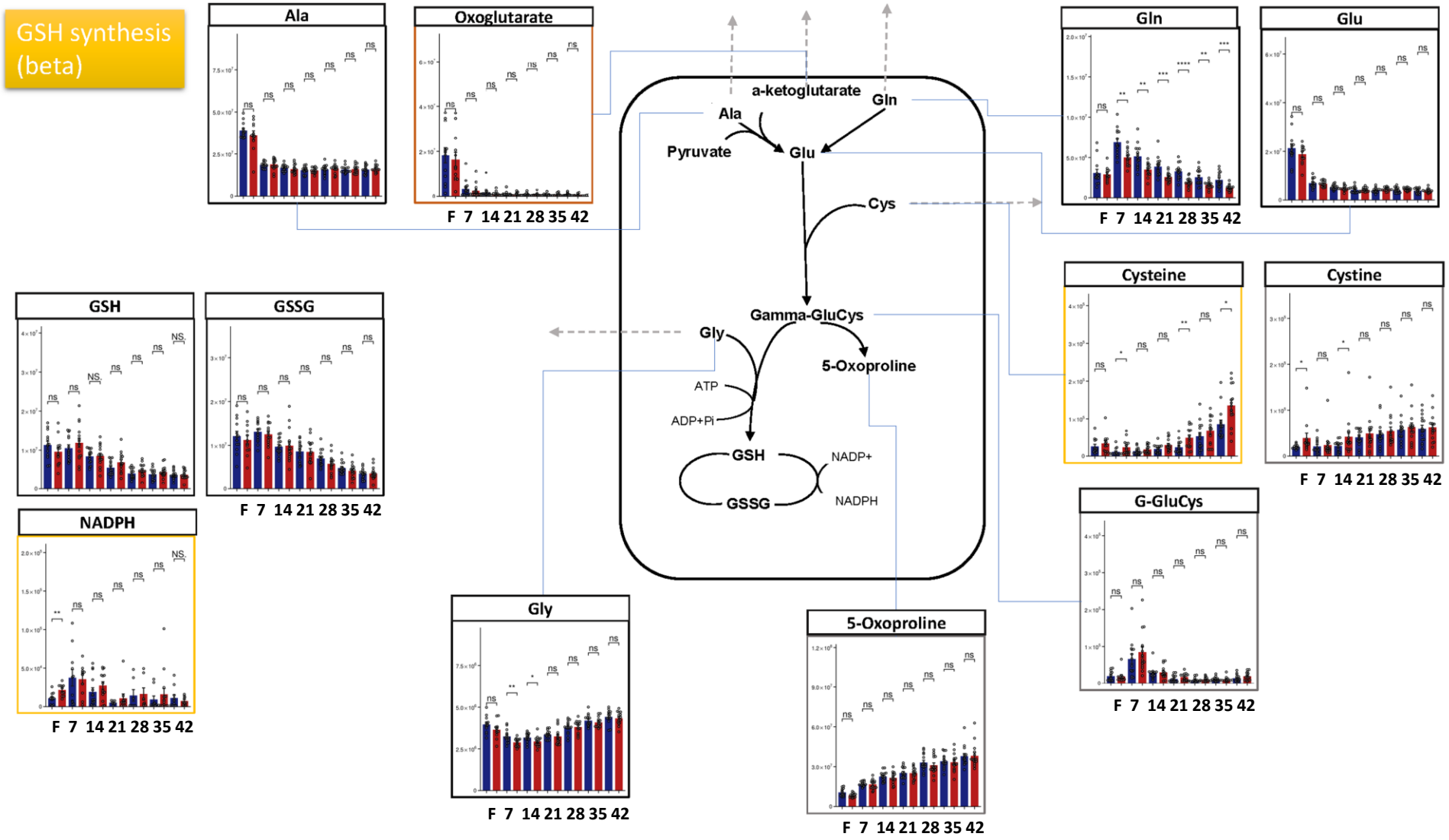

Supplementary Figure S8. Bar plots of metabolites in glutaminolysis and transamination pathways in control (blue) and βThal$^+$ (red) RBCs *in vivo* (fresh blood, F) and weekly through storage (days 7, 14, 21, 28, 35 and 42). (*), (**), (***), (****): p< 0.05, 0.01, 0.001, 0.0001 βThal$^+$ vs. control, respectively.

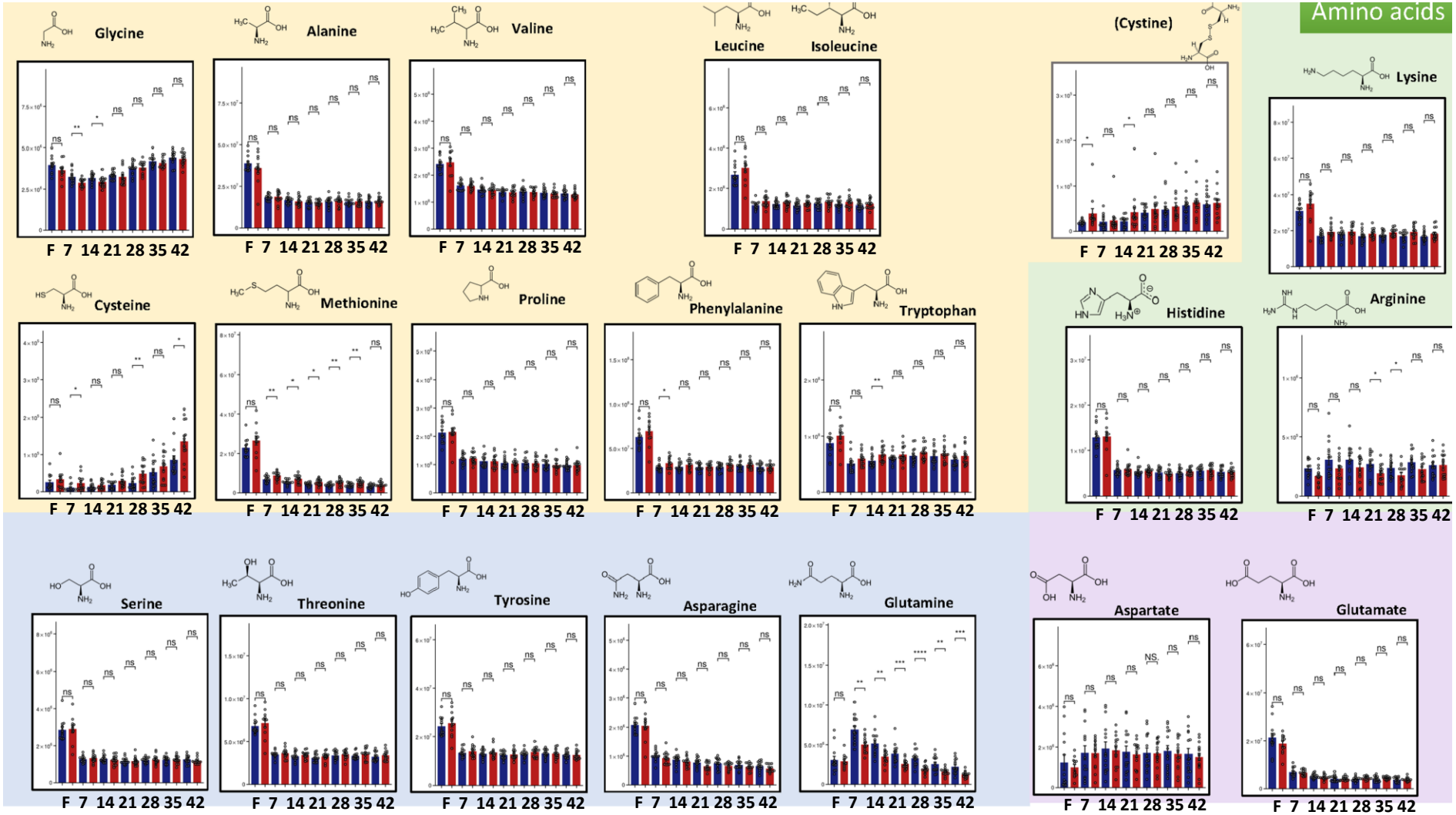

Supplementary Figure S9. Bar plots of amino acids in control (blue) and βThal⁺ (red) RBCs *in vivo* (fresh blood, F) and weekly through storage (days 7, 14, 21, 28, 35 and 42). (*), (**), (***), (****): p< 0.05, 0.01, 0.001, 0.0001 βThal⁺ vs. control, respectively.

Free Fatty Acids

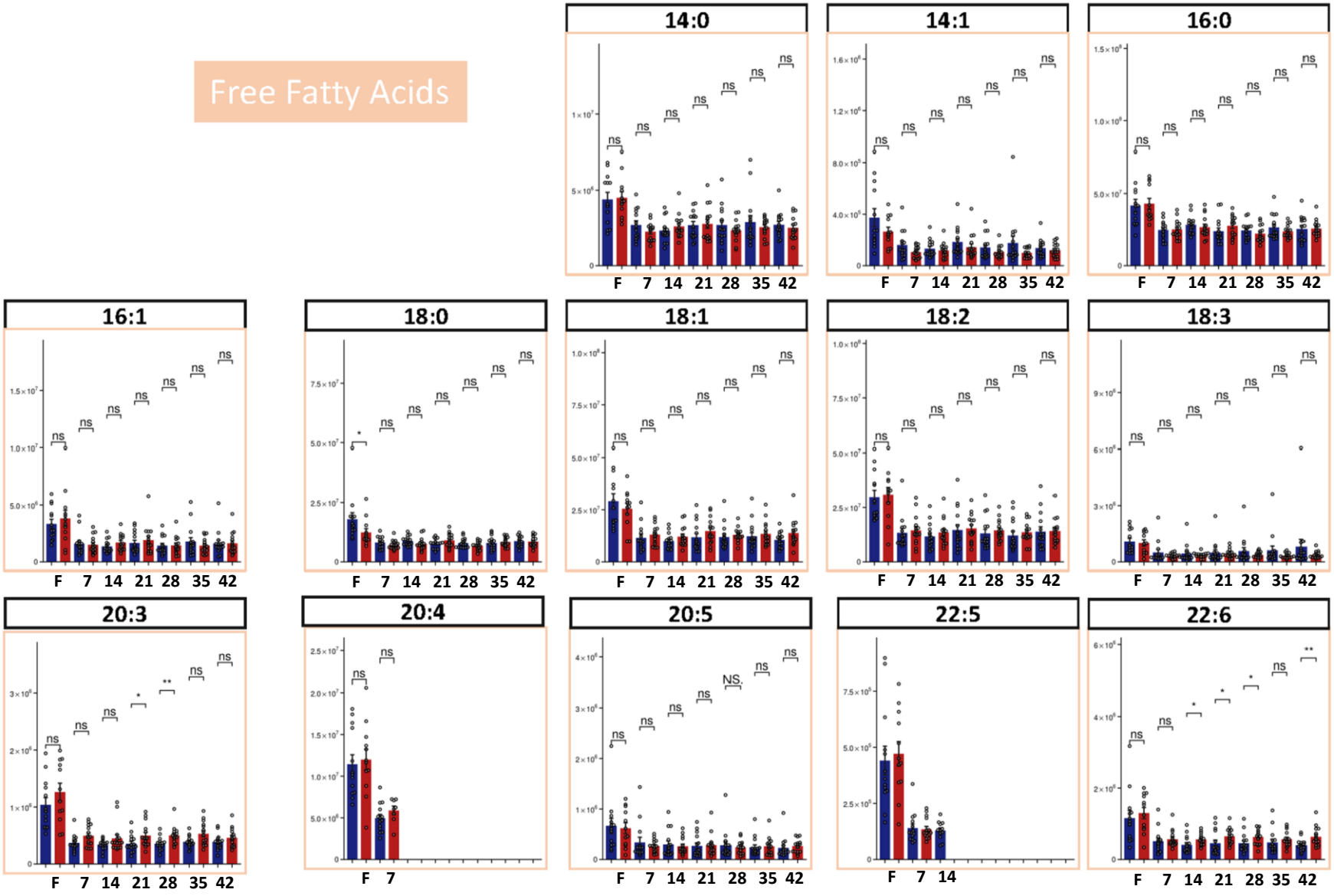

Supplementary Figure S10. Bar plots of free fatty acids in control (blue) and βThal^{+} (red) RBCs *in vivo* (fresh blood, F) and weekly through storage (days 7, 14, 21, 28, 35 and 42). (*), (**), (***), (****): p< 0.05, 0.01 βThal^{+} vs. control, respectively.

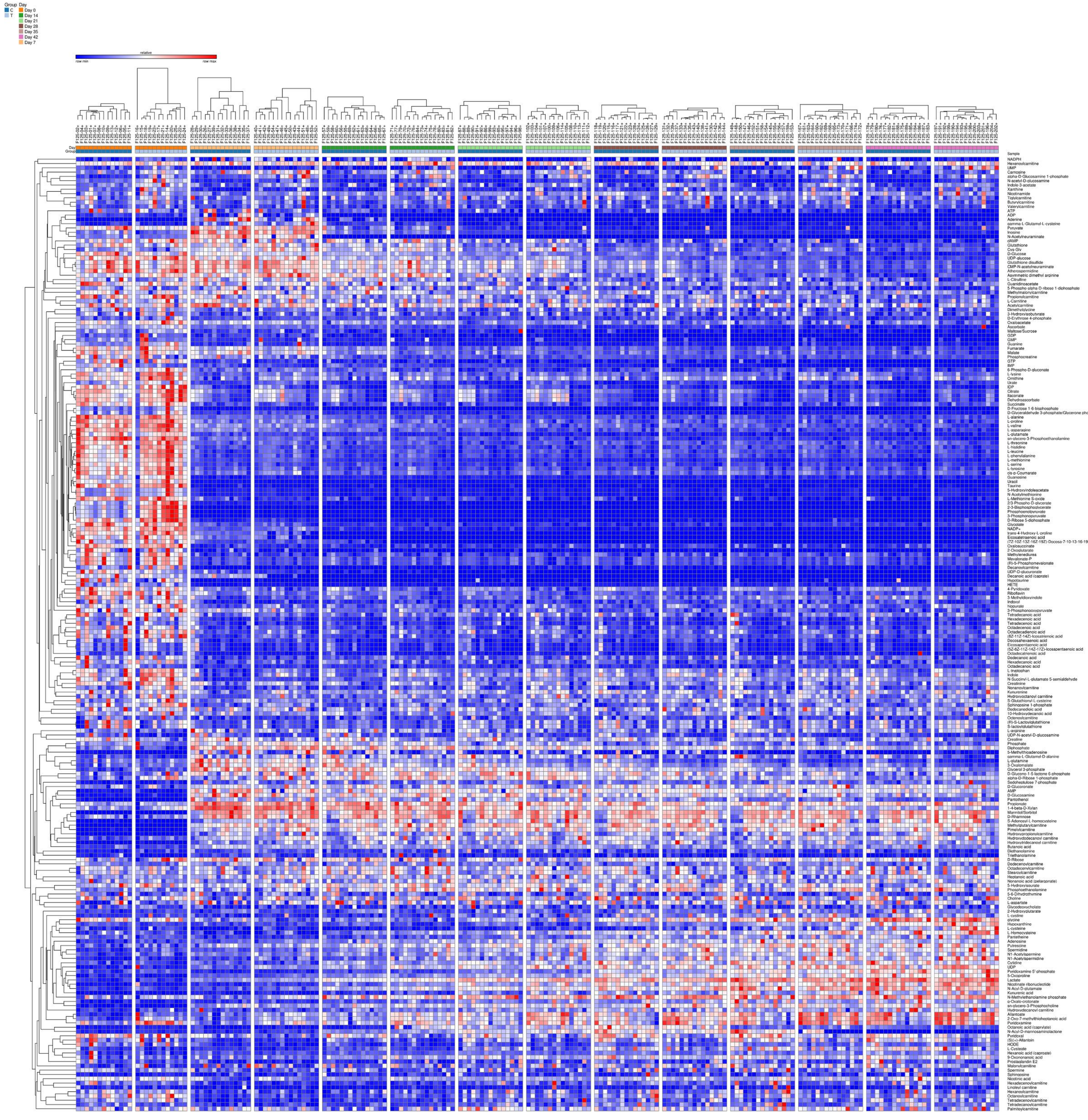

Supplementary Figure S11. Heatmap of full metabolomics analyses performed in paired fresh (Day 0) and stored (Days 7, 14, 21, 28, 35, 42) RBCs from the control and ϐThal$^+$ groups (n=13 or 12 for Day 0 control and ϐThal$^+$ RBC samples, respectively; n=15 per group for the stored RBC samples).

Supplementary References

1. Benzie IF, Strain JJ. The ferric reducing ability of plasma (FRAP) as a measure of "antioxidant power": the FRAP assay. Anal Biochem. 1996;239(1):70-76.
2. Duplancic D, Kukoc-Modun L, Modun D, Radic N. Simple and rapid method for the determination of uric acid-independent antioxidant capacity. Molecules. 2011;16(8):7058-7068.
3. Pallotta V, Gevi F, D'Alessandro A, Zolla L. Storing red blood cells with vitamin C and N-acetylcysteine prevents oxidative stress-related lesions: a metabolomics overview. Blood Transfus. 2014;12(3):376-387.
4. Tzounakas VL, Kriebardis AG, Georgatzakou HT, et al. Glucose 6-phosphate dehydrogenase deficient subjects may be better "storers" than donors of red blood cells. Free Radic Biol Med. 2016;96:152-165.
5. Thomas T, Stefanoni D, Dzieciatkowska M, et al. Evidence for structural protein damage and membrane lipid remodeling in red blood cells from COVID-19 patients. medRxiv. 2020.
6. Reisz JA, Chessler KM, Dzieciatkowska M, D'Alessandro A, Hansen KC. Blood and Plasma Proteomics: Targeted Quantitation and Posttranslational Redox Modifications. Methods Mol Biol. 2017;1619:353-371.
7. Nemkov T, Reisz JA, Gehrke S, Hansen KC, D'Alessandro A. High-Throughput Metabolomics: Isocratic and Gradient Mass Spectrometry-Based Methods. Methods Mol Biol. 2019;1978:13-26.
8. Nemkov T, Hansen KC, D'Alessandro A. A three-minute method for high-throughput quantitative metabolomics and quantitative tracing experiments of central carbon and nitrogen pathways. Rapid Commun Mass Spectrom. 2017;31(8):663-673.
9. Clasquin MF, Melamud E, Rabinowitz JD. LC-MS data processing with MAVEN: a metabolomic analysis and visualization engine. Curr Protoc Bioinformatics. 2012;Chapter 14:Unit14 11.